ISSN 1392–1207. MECHANIKA. 2022 Volume 28(4): 329–337

Development and Comparative Evaluation of Reduced-scale Krauss Friction Tester based on Similarity Theory

Zhenyu WANG*, Jie WANG, Lining WANG***, Yunhai MA******

**School of Automation, Chengdu University of Information Technology, Chengdu 610065, China,*
E-mail: wangzhenyu2009@163.com (Corresponding author)
***School of Manufacturing Science and Engineering, Sichuan University, Chengdu 610065, China*
****College of Biological and Agricultural Engineering, Jilin University, Changchun 130022, China*
*****College of Biological and Agricultural Engineering, Jilin University, Changchun 130022, China*

crossref http://dx.doi.org/10.5755/j02.mech.32030

1. Introduction

Among brakes, clutches and driving devices of many vehicles, friction composites make up important parts [1, 2]. The reliability and stability of the executive components are directly linked with friction composites [3]. Hence, suitable friction coefficients and better wear resistance under various temperatures and complex conditions must be presented [4]. The friction composites should no noise and vibration-free during working, and consist of eco-friendly ingredients. So they are usually made up of over ten ingredients, such as resin binder, fibres, abrasive fillers, Lubricating or antifriction agent, and quality modifiers [5 –7]. These fibres reinforced materials play a key role in improving mechanical strength and preventing all kinds of damage [8 – 11].

Numerous friction and wear testing means for these friction composites are quite popular globally, one is full-scale friction testers [12], such as brake-dynamometer tester [13, 14], Krauss tester [15], the other is a small sample friction tester, such as FAST tester, Chase tester [16], Constant speed tester [17] etc. Among these testing machines, the Krauss tester had originated in Germany and was developed by ATE-TEVES and ERICH.KRAUSS. This Krauss tester had been widely used in the field of friction material examination in Europe, and been recognized as the authoritative equipment for evaluating the performance of automotive brake friction materials. A number of researchers [18 - 22] used the Krauss friction tester to evaluate the friction and wear properties of friction composites.

Since the small sample friction testers and the full-scale friction testers have performed different test procedures, different simulation conditions and different evaluation methods, their test data are completely different, so they are difficult to have uniform and similar results. The small sample friction testers such as Chase and FAST are mainly considered as a quality control test in the laboratory to obtain material component properties [23]. The full-scale friction testers such as Brake-Dynamometer and Krauss can truly simulate various working conditions, and can obtain more realistic experimental data for evaluating product quality. Similarity theory is a reliable method to establish a close relationship between the small sample friction testers and the full-scale friction testers. In recent years, similarity theory has been widely applied to different fields such as structural engineering, vibration and shock issues. It can help researchers reliably predict the performance of the prototype [24, 25]. Luo et al. [26] proposed a design method of similarity model considering the requirement of static strength and established dynamic similarity relation by using equation analysis method. Wang et al. [27] designed a 1/2 scale lunar rover model based on similarity theory. The slope angle and wheel velocity were taken as the experimental factors, the wheel sinkage and slip ratio were taken as the experimental index, test on lunar rover's slope trafficability was carried out. Through finite element simulation and small model impact test, Wang et al. [28] demonstrated the feasibility of analyzing the energy absorption characteristics of the axial impact process of aluminum foam based on similarity theory. Wang et al. [29] performed a comparative experiment of vibrating screen model and prototype based on similarity theory, which verified the consistency and reliability of prototype and model. Guo et al. [30] deduced the similitude criteria for steady operation and non-steady operation of externally pressurized spherical gas bearing with inherent compensation. The results of theoretical analysis were consistent with the numerical calculation. Based on the similarity theory, foreign scientists Sanders et al. [31] had developed a reduced-scale inertial brake dynamometer. The testing machine had designed one sliding friction surface and matched two friction specimens, which had been manufactured and examined by the link company. The test results showed that the agreement between testing machines was excellent and the minimal friction variability was displayed. Engineers Zhao et al [32] had developed a reduced-scale brake dynamometer, which provide a single friction surface to match a single sample. Comparative test results indicated that their friction coefficients have the same trend in the whole experiment process. Researchers Ma et al. [33] had manufactured an inertial reduced-scale friction test device. Based on the above research, Krauss GMBH of Germany and Jilin University Mechanical and Electrical Equipment Research Institute jointly proposed the idea of developing a reduced-scale Krauss friction tester, which has been reported to ISO organization.

2. Scaling

2.1. Similarity criterion for braking components in friction process

If there are n physical quantities in a physical phenomenon, and $\varphi(x_1, x_2, x_3,\ldots,x_n)=0$. There are m basic physical quantities, and their dimensions are independent of each other. Then these n physical quantities can be expressed as a functional relationship between n-m similarity criteria π_1,

π_2, π_3,…, π_{n-m}. That is, $f(\pi_1, \pi_2, \pi_3,\ldots, \pi_{n-m}.)=0$. The dimension of the main physical quantity in the friction process had been selected, and the relationship between the physical quantities had been established according to the similar second theorem, then:

$$f\left(\mu, E, A, P, F, L, T, M, R, D\right)=0. \tag{1}$$

Where, the physical quantities are as shown in Table 1. In order to facilitate the dimension analysis, braking force F; length L and braking time T are taken as three basic dimensions. Using the dimension matrix analysis method, the expressions of the relevant physical quantities in the force system are shown in Table 1.

Table 1

The dimensionless expression of the relative physical quantity in the force system

Physical quantity	Symbol	Dimension
Friction coefficient	μ	$F^0L^0T^0$
Elastic modulus of friction disk	E	FL^{-2}
Pad area	A	L^2
Pad pressure	P	FL^{-2}
Braking force	F	F
Length	L	L
Braking time	T	T
Friction torque	M	FL
Effective radius	R	L
Friction disc diameter	D	L

Its π term is:

$$\pi=\mu^a E^b A^c P^d F^e L^f T^g M^h R^j D^k, \tag{2}$$

where: a, b, c, d, e, f, g, h, j, represents the indices of μ, E, A, P, F, L, T, M, R, D respectively, the dimensional matrix of the system is:

$$\begin{bmatrix} & a & b & c & d & e & f & g & h & j & k \\ & \mu & E & A & P & F & L & T & M & R & D \\ F & 0 & 1 & 0 & 1 & 1 & 0 & 0 & 1 & 0 & 0 \\ L & 0 & -2 & 2 & -2 & 0 & 1 & 0 & 1 & 1 & 1 \\ T & 0 & 0 & 0 & 0 & 0 & 0 & 1 & 0 & 0 & 0 \end{bmatrix}. \tag{3}$$

According to the relationship between the indices, the following equations are obtained:

$$\begin{cases} b+d+e+h=0 \\ -2b+2c-2d+f+h+j+k=0. \\ g=0 \end{cases} \tag{4}$$

After transformation, the following equations:

$$\begin{cases} e=-d-h \\ f=-b-2c+2d-h-j-k. \\ g=b \end{cases} \tag{5}$$

According to the similarity theorem, the π matrix of each parameter of the braking process is obtained.

$$\begin{bmatrix} & a & b & c & d & h & j & k & e & f & g \\ & \mu & E & A & P & M & R & D & F & L & T \\ \pi_1 & 1 & 0 & 0 & 0 & 0 & 0 & 0 & 0 & 0 & 0 \\ \pi_2 & 0 & 1 & 0 & 0 & 0 & 0 & 0 & -1 & 2 & 0 \\ \pi_3 & 0 & 0 & 1 & 0 & 0 & 0 & 0 & 0 & -2 & 0 \\ \pi_4 & 0 & 0 & 0 & 1 & 0 & 0 & 0 & -1 & 2 & 0 \\ \pi_5 & 0 & 0 & 0 & 0 & 1 & 0 & 0 & -1 & -1 & 0 \\ \pi_6 & 0 & 0 & 0 & 0 & 0 & 1 & 0 & 0 & -1 & 0 \\ \pi_7 & 0 & 0 & 0 & 0 & 0 & 0 & 1 & 0 & -1 & 0 \end{bmatrix}. \tag{6}$$

Each dimension of the above π matrix represents the power of each parameter. The power of the same row in a matrix constitutes a π factor. The seven similarity criterions $\pi_1 \sim \pi_7$ are obtained in turn as follows: $\pi_1=\mu$; $\pi_2=\frac{(EL^2)}{F}$; $\pi_3=\frac{A}{L^2}$; $\pi_4=\frac{PL}{F}$; $\pi_5=\frac{M}{FL}$; $\pi_6=\frac{R}{L}$; $\pi_7=\frac{D}{L}$.

2. 2. Derivation of the similarity ratio of each parameter

It is assumed that the similarity ratio between the parameters of the prototype and the similar model during braking is expressed as: $\frac{\mu_p}{\mu_m}=C_\mu$; $\frac{E_p}{E_m}=C_E$; $\frac{A_p}{A_m}=C_A$; $\frac{P_p}{P_m}=C_P$; $\frac{M_p}{M_m}=C_M$; $\frac{R_p}{R_m}=C_R$; $\frac{D_p}{D_m}=C_D$; $\frac{F_p}{F_m}=C_F$; $\frac{L_p}{L_m}=C_L$; $\frac{T_p}{T_m}=C_T$. Where p is prototype and m is model.

The scaling model of the brake assembly is similar to its prototype in terms of geometry and boundary conditions. Based on the physical object of the brake component, the geometric size of the scaling model is enlarged or reduced according to the scale factor. That is $\frac{L_p}{L_m}=C_L=\lambda$, where λ is scale factor.

It is assumed that the time T required for each brake and the pad pressure P should be the same. Then $C_T=1$, $C_P=1$. Other scale factor between the model and the prototype can be obtained: $C_\mu=1$; $C_A=\lambda^2$; $C_F=\lambda^2$; $C_M=\lambda^3$; $C_R=\lambda$; $C_D=\lambda$.

3. Reduced-scale Krauss machine design

3. 1. Basic parameters

For the selection of the scale coefficient, different technical fields had different requirements, and this coefficient was selected according to the specific conditions of the test. In general, the smaller the scale coefficient was, the smaller the model was, the volume of the device would be reduced and the test error would be larger. Increasing the scale coefficient could improve the testing accuracy, and if the coefficient was larger, its value will be greatly weakened. In the field of tribology, it was necessary to ensure that the friction linear velocity of the reduced-scale test machine

was the same as that of the original test machine, and the smaller the friction radius, the higher the friction disk rotational speed and the higher the manufacturing precision. The scale factor of the reduced-scale inertia dynamometer studied in the previous study was 1:4 or 1:5 [31 – 32, 34]. The friction area of the Mercedes-Benz brake liner installed on the full-scale Krauss tester was about 88 cm^2. The pad area of the small sample testing machine such as the constant speed friction testing machine is 6.25 cm^2, and the Chase is 6.45 cm^2 [35]. The size of the friction specimen was usually taken as an integer to facilitate the preparation of the sample. This proportional coefficient also determines the size of the brake disc. If the brake disc was too small, it was easy to cause manufacturing and installation problems. For ease of calculation, the pad area ratio of reduced-scale model to full-scale product is given as 1:4.4, that is $C_A=\lambda^2=4.4$. The size of the reduced-scale sample was exactly 44×25 mm. The geometric scaling ratio of the model is obtained, $\lambda=\sqrt{C_A}\approx 2$. Many parameters of the Krauss testing machine are determined according to the Mercedes disc brake. The basic parameters of the reduced-scale Krauss tester are determined, as shown in Table 2.

Table 2

Basic parameters of reduced-scale Krauss tester

Parameters	Symbol	Scale	Value	Units
Sliding speed	*v*	1:2	7.46	m/s
Pad area	*A*	1:4.4	10	cm^2
Pad pressure	*P*	1:1	10	bar
Braking force	*F*	4.4:1	1003	N
Braking time	*T*	1:1	5	s
Effective radius	*R*	1:2	54	mm

3. 2. Structure and composition

The reduced-scale Krauss tester for tribological evaluation of brake friction materials should be able to simulate operating conditions such as sliding speed, contact pressure and temperature etc. As shown in Fig. 1, the reduced-scale Krauss tester is mainly composed of power system, temperature measurement system, speed measurement system, braking system, servo loading system, torque measurement system and cooling and dust-removal system. The power system is equipped with a 15 kw motor that drives the main shaft to rotate through a belt. The friction disc is fixed at the end of the main shaft. The temperature measurement system can measure the temperature of the disc and the pad during the experiment. The speed measurement system is used to accurately measure the rotation speed of the main shaft. The friction torque is obtained by the pressure sensor in the torque measurement system. Brake pad pressure is provided by the servo loading system. In the cooling and dust-removal system, the brake disc is cooled by the blower through the air supply pipe, and the heat and dust are discharged by the exhaust fan through the exhaust duct. It can not only control the test temperature well, but also keep the brake system and the inside clean.

The braking system structure is shown in Fig. 2. The braking system is designed with reference to the Mercedes disc brakes, which can greatly enhance the accuracy of the comparison test. The whole assembly is mainly divided into two parts, which is named left caliper body and right caliper body. The boss on the upper part of the left caliper body is connected to the braking arm. The exhaust hole and oil entrance are respectively arranged in the top and the bottom of the two caliper bodies. The specimen clamp is placed in the middle of the brake caliper, and the specimen is installed in its cavity. The ring handle is designed to facilitate the specimen clamp to be removed and placed from the caliper body. The caliper body is made into a hydraulic cylinder body, in which a piston is installed and sealed through a sealing ring. The friction disc is located in the middle of the two specimen clamps and is connected to the main shaft by means of a flange.

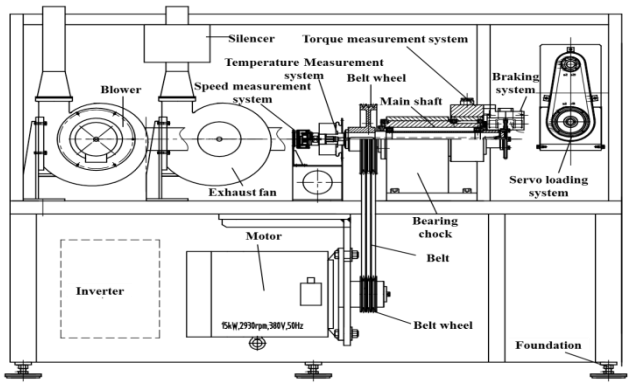

Fig. 1 Diagram for the reduced-scale tester

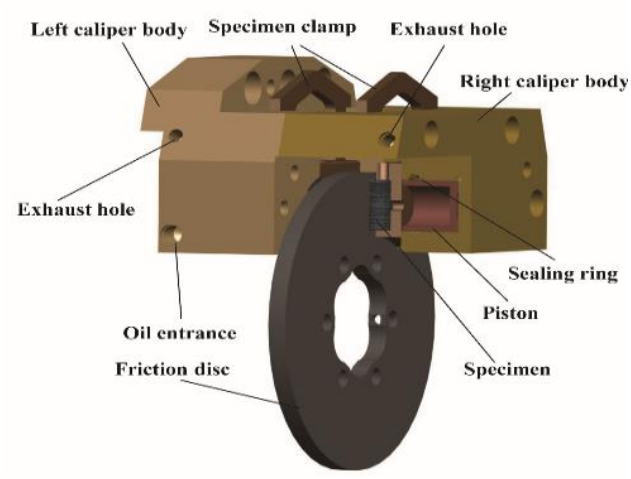

Fig. 2Diagram of braking system

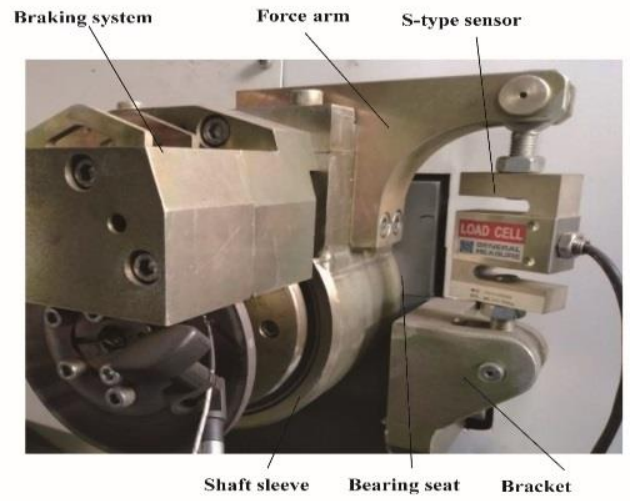

Fig. 3 Diagram of torque measurement system

As shown in Fig. 3, the torque measurement system is closely connected to the braking system. The shaft sleeve is fixedly connected to the left caliper body and the

force arm. The bearing is mounted between the shaft sleeve and the main shaft. When the main shaft rotates, the shaft sleeve does not rotate with it. During the braking process, the generated friction torque is transmitted to the shaft sleeve through the left caliper body and measured by the S-type sensor. The upper end of the S-type sensor is articulated with the force arm, and the lower end is supported on the bracket of the bearing seat.

The designed brake disc (Fig. 4) is fully-pearlitic cast iron disk, which has the same composition and microstructure as Mercedes-Benz brake disc with hardness of HB170 to HB190. The main ingredients and content are shown in Table 3. The microstructure of the material is pearlite > 98 %, ferrite < 2 %. Blowhole, impurities, shrinkage porosity, cracks and other defects are not allowed in the casting process.

Fig. 4 Dimensions and factual picture of friction disc

Table 3

Ingredients and content of the friction disk

C	Si	Mn	Ni	Cr	P	S
3.5~ 4.0	2.0~ 2.4	0.6~ 1.0	0.6~ 0.7	0.15~ 0.25	<0.1	<0.1

The detailed structure of the reduced-scale Krauss tester is illustrated in Fig. 5. During the test, the speed is measured by the speed sensor, the output torque is provided by the torque sensor, and the pressure sensor shows the brake pressure signal. According to the test standard, the thermocouple which is closely attached to the surface of the friction disc is used to collect the temperature signal. The detailed structure of the full-scale Krauss tester is illustrated in Fig. 6. The motor and the spindle are directly connected by flanges, Full-scale brakes were selected. The temperature was adjusted by air conditioning. The torque was measured by a sensor on the sliding table. The pressure loading and temperature measurement are the same as the reduced-scale Krauss tester.

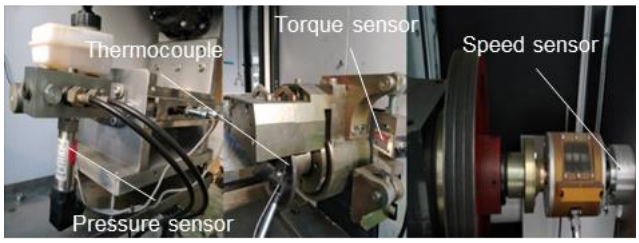

Fig. 5 Detailed structure for the reduced-scale Krauss tester

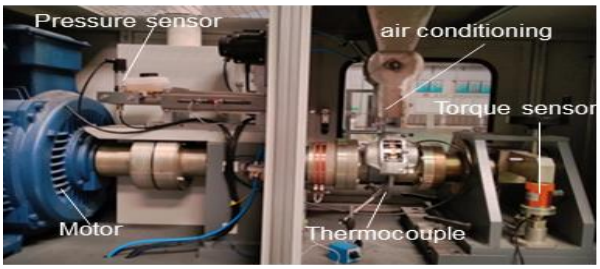

Fig. 6 Detailed structure for the full-scale Krauss tester

4. Experimental

4.1. Test procedure

In order to evaluate the performance of the reduced-scale Krauss tester, the international ECE R-90 test procedure was used to compare with the full-scale Krauss tester. The main test procedures for the ECE R-90 are indicated in Table 4. The test procedure has a total of 12 brake sequence. The pilot project consists mainly of bedding, cooling cycle, fade, recovery and thermal performance. A total of 84 consecutive brake applications were carried out during the whole test process. Each brake application has a braking interval of 5 seconds brake applied followed by 10 seconds brake released. During the braking time of 5s, data is collected approximately one time per 2ms, and nearly 2500 sets of data are collected for each brake application.

Table 4

E R-90 test procedure

Brake sequence	Test section	Brake cycle	Number of brake applications	rpm		Pressure (Bar)		Initial brake temperature, °C	Forced cooling
				Full-scale	Reduced-scale	Full-scale	Reduced-scale		
1	bedding	1-6	5	660	1229	15.6	19.8	100	yes
2	cooling cycle	7	5	660	1229	15.6	19.8	100	yes
3	fade	8	5	660	1229	15.6	19.8	≤150	no
4	fade	9	5	660	1229	15.6	19.8	200	no
5	fade	10	5	660	1229	15.6	19.8	≤250	no
6	fade	11	5	660	1229	15.6	19.8	300	no
7	recovery	12	3	660	1229	15.6	19.8	250	yes
8	recovery	13	3	660	1229	15.6	19.8	200	yes
9	recovery	14	3	660	1229	15.6	19.8	150	yes
10	recovery	15	10	660	1229	15.6	19.8	100	yes
11	thermal performance	16	5	660	1229	15.6	19.8	≤250	no
12	thermal performance	17	5	660	1229	15.6	19.8	300	no

4.2. Results and discussion

Comparison of experimental data obtained from reduced-scale and full-scale Krauss tester was performed. The results of friction torque *M*, braking pressure *P*, test

temperature *T*, friction coefficient μ and test time were compared and analyzed.

4.2.1. Comparison of friction torque and pressure

When the temperature is close to 250 °C, the resin binder in the friction material will decompose at high temperature. During this process, the friction coefficient of the brake friction material will decrease, resulting in a reduction in the braking friction torque. Subsequently, the friction material has been solidified, the friction coefficient is increased, and the recovery process begins. In this process, the braking torque increases and the fluctuations range decreases. In the fade and recovery phases, single brake application with an initial brake temperature of 250 °C was selected, and the friction torque and brake pressure were compared and analyzed. The comparison results are shown in Fig. 7, the same pressure-controlled had been chosen for analysis in the whole process.

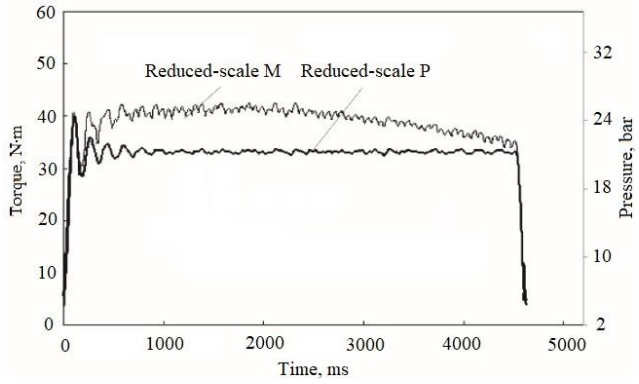

a

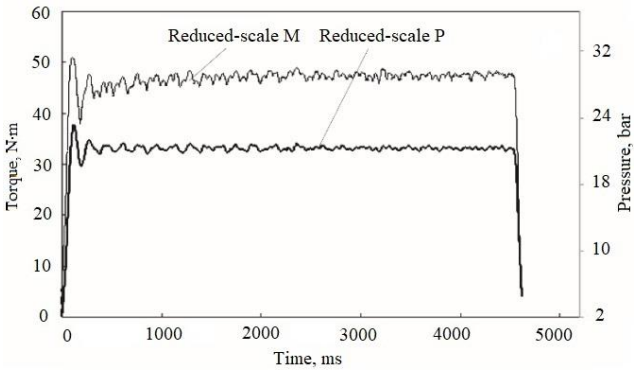

b

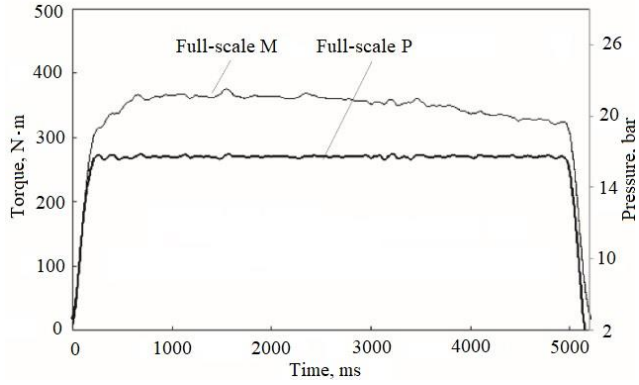

c

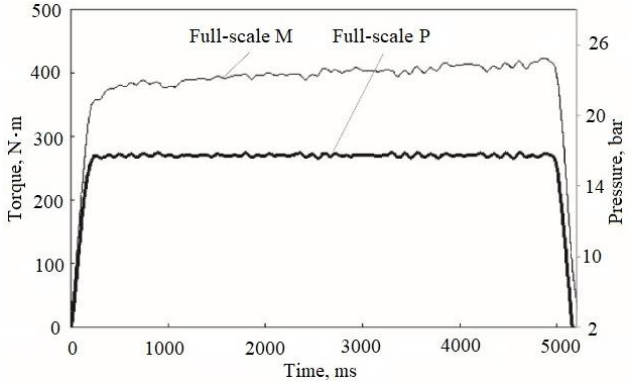

d

Fig. 7 Comparison of friction torque and pressure results during fade and recovery at 250°C: a) Friction curve of the reduced-scale Krauss tester in the fade stage; b) Friction curve of the reduced-scale Krauss tester in the recovery stage; c) Friction curve of the full-scale Krauss tester in the fade stage; d) Friction curve of the full-scale Krauss tester in the recovery stage

Each brake application of the vehicle is roughly divided into three processes, brake growth process, main brake process, and a brake release process. As illustrated in Fig. 7a and 7b, during the braking growth process, brake pressure and torque curves of the reduced-scale Krauss tester experienced the process of rapid ascent, concussion finishing and stabilization. The main reason for this phenomenon was that the brake piston diameter of reduced-scale and full-scale Krauss tester was about 1:2.36. Since the piston diameter and working volume of the hydraulic oil are smaller, in addition, the small piston has a relatively smaller motion drag, so the pressure rises rapidly. Then the vibration of the pressure was adjusted, the fluctuation range was gradually reduced, and finally the braking pressure was close to the given value. In the same way, during the brake release process, the small piston responded quickly and moved rapidly, so each stop time was about 4630 ms, 370 ms earlier than the given value. As can be seen from Figs. 7(c) and (d), there is no loading fluctuation in the friction torque and brake pressure of the full-scale Krauss tester during the brake growth process. Due to larger piston diameter, slower motion response and greater motion drag, each stop time is approximately 5240 ms, which is 240 ms behind the given value.

4.2 2. Comparison of friction coefficient

As can be seen from Fig. 8, the two groups of friction coefficient data have the same changing trend during the test. The average coefficient of friction of the reduced-scale Krauss test during the whole test was 0.473, and that of the full-scale Krauss test was 0.443. Their average friction coefficient was close, and the relative error was only 6.3%. It can be seen from the figure that the fluctuation range of friction coefficient of full-scale Krauss test was greater than that of reduced-scale Krauss test. The results showed that in the fade section, the minimum friction coefficient appeared in the 55th brake, the values of full-scale and reduced-scale is 0.219 and 0.427 separately. The maximum friction coefficient appeared in the 57th brake in the recovery phase, the value of full-scale and reduced-scale was 0.578 and 0.567 separately.

4.2.3. Comparison of test temperature

The disk temperature was selected in the ECE R-90 test procedure. As can be seen from Fig. 9, the temperature agreed well between the reduced-scale and full-scale Krauss tester. Fig. 10 exhibits the results of correlation analysis between two test temperature data. The linear fitting curve equation of the test temperature was obtained as y = 1.138x-40.61, and R^2 = 0.972, indicating that test temperatures of two tester had a good linear correlation.

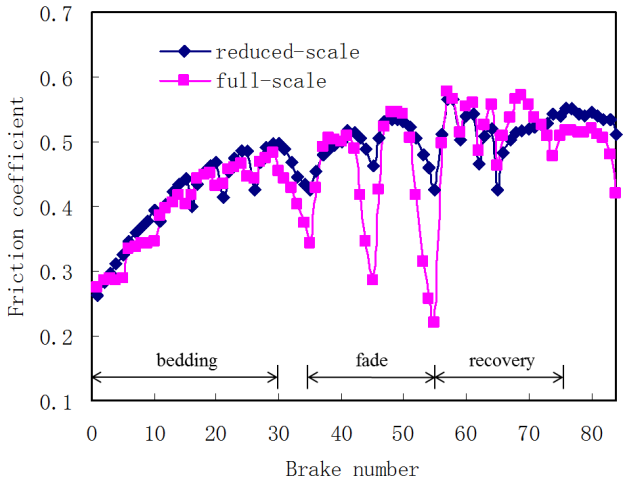

Fig. 8 Comparison chart between average friction coefficient

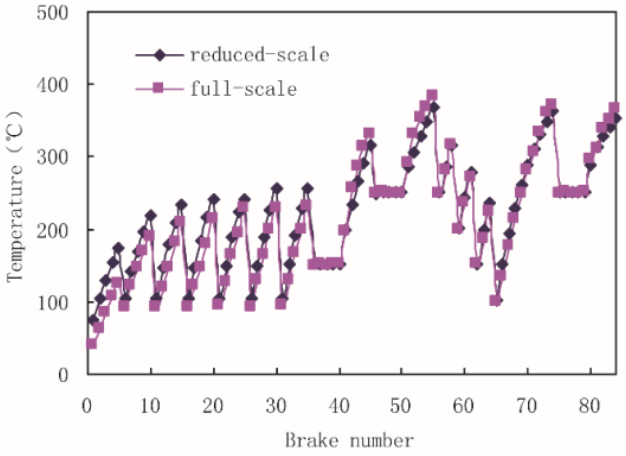

Fig. 9 Comparison chart between test temperatures

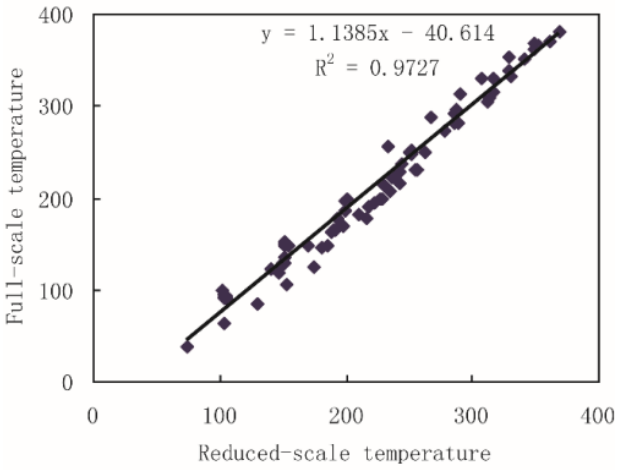

Fig. 10 Relationship between test temperatures

4.2.4. Comparison of test time and cost

The average value of each brake time of the reduced-scale and full-scale Krauss tester is 4.62 s and 5.24 s respectively. As shown in Fig. 11, with the increased of brake numbers, the accumulative test time difference between the two Krauss testers increased gradually. The more brake numbers, the greater the cumulative brake time difference. After the test, the cumulative test time for reduced-scale and full-scale Krauss tester was 3877.9 s and 4793.6 s, respectively. The total test time for reduced-scale Krauss tester was about 4/5 of full-scale Krauss tester.

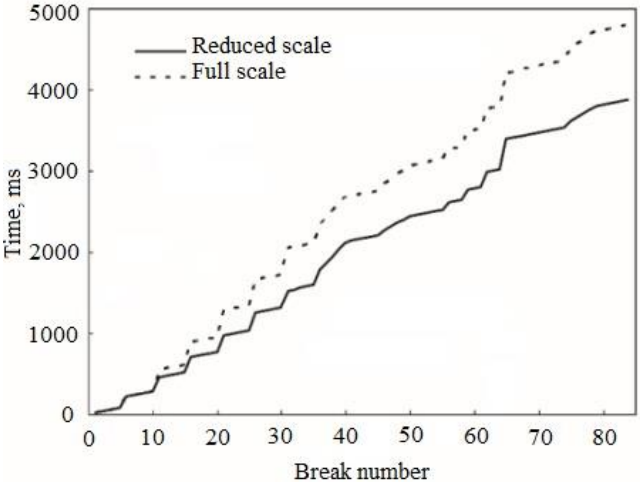

Fig. 11 Comparison chart between accumulative test time

During the test, the motor power consumption is mainly divided into two parts, which can be calculated as follows:

$$W = W_1 + W_2, \tag{7}$$

where: W is the total power consumption of the motor; W_1 is the power consumption of the brake applied time; W_2 is the total power consumption of the brake release time.

It is assumed that the active loss is converted into friction work in each brake applied. In the process of brake release, the reactive power loss is about 10 % of the rated power. Then:

$$W_1 = \sum_{k=1}^{m} P_{1k} t_{1k} = \frac{T\pi n}{30\eta} t_a \cdot m, \tag{8}$$

$$W_2 = \sum_{k=1}^{m} P_{2k} t_{2k} \approx 10\% P_N t_b \cdot m, \tag{9}$$

where: P_{1k} is the power loss of each brake applied; t_{1k} is each brake applied time; P_{2k} is the reactive power loss of each brake release; $t_{2k}$is each brake release time; T is the average torque of the test machine; n is the rotation speed of the test machine; t_a is the average time of each brake applied; t_b is the average time of each brake release; m is the number of brake applied or release; P_N is the rated power of the motor; η is the motor efficiency.

Then the ratio of the power consumption of the motor is:

$$\frac{W_R}{W_F}=\frac{\frac{T_R\pi n_R}{30\eta}t_{Ra}+10\%P_{RN}t_{Rb}}{\frac{T_F\pi n_F}{30\eta}t_{Fa}+10\%P_{FN}t_{Fb}}=\frac{T_R\pi n_R t_{Ra}+3\eta P_{RN}t_{Rb}}{T_F\pi n_F t_{Fa}+3\eta P_{FN}t_{Fb}}. \quad (10)$$

The subscript *R* represents reduced-scale Krauss tester parameters; subscript *F* represents full-scale Krauss tester parameters. The known parameters are shown in Table 5.

It was known by calculation that if the same other conditions existed, the power cost of the reduced-scale Krauss tester was 20.79 % of the power cost of the full-scale Krauss tester when the ECE R-90 test program was executed. It could be concluded that the reduced-scale Krauss test had great potential to reduce test time and cost.

Table 5

Krauss tester parameters

T_R, N·m	T_F, N·m	n_R, r/min	n_F, r/min	P_{RN}, KW	P_{FN}, KW	t_{Ra}, s	t_{Rb}, s	t_{Fa}, s	t_{Fb}, s	η
43.8	345.9	1229	660	15	75	4.62	10.38	5.24	9.76	

5. Conclusions

Based on the similarity principle, the reduced-scale Krauss tester had been designed and manufactured. The same batch and molded NAO brake friction material had been rigorously evaluated on two Krauss testers following ECE R-90 procedure. The comparative evaluation results of the testing machine showed that the reduced-scale Krauss tester was faster response than that of the full-scale Krauss tester in the process of brake growth and brake release, the average value of each brake time of the reduced-scale and full-scale Krauss tester is 4.62 s and 5.24 s respectively. During the entire test, the average coefficient of friction was closer and the relative error is 6.3 %, and the maximum and minimum values of the friction coefficient appeared at the same brake sequence, test section and brake cycle. The test temperature had good linear correlation in the whole test process. In each test, the power cost of the reduced-scale Krauss tester was 20.79 % of the power cost of the full-scale Krauss tester when the ECE R-90 test program was executed. It could be concluded that the reduced-scale Krauss test had great potential to reduce test time and cost.

Acknowledgments

This work was financially supported by National Science Foundation of China (51279206), Leshan Science and Technology Project Foundation (20ZDYJ0135)

References

1. **Ji, Z.; Jin, H.; Luo, W.** 2017. The effect of crystallinity of potassium titanate whisker on the tribological behavior of NAO friction materials, Tribology International 107: 213-220. http://dx.doi.org/10.1016/j.triboint.2016.11.022.
2. **Polajnar, M.; Kalin, M.; Thorbjornsson, I.** 2017. Friction and wear performance of functionally graded ductile iron for brake pads, Wear 382–383: 85-94. http://dx.doi.org/ 10.1016/j.wear.2017.04.015.
3. **Ingram, M.; Spikes, H.; Noles, J**. 2010. Contact properties of wet clutch friction material, Tribology International 43(4): 815-821. http://dx.doi.org/ 10.1016/j.triboint.2009.11.008.
4. **Kuroe, M.; Tsunoda, T.; Kawano, Y.; Takahashi, A.** 2013. Application of lignin-modified phenolic resins to brake friction material, Journal of Applied Polymer Science 129(1): 310-315. http://dx.doi.org/ 10.1002/app.38703.
5. **Yun, C. K.; Min, H. C.; Seong, J. K., Ho, J.** 2008. The effect of phenolic resin, potassium titanate, and CNSL on the tribological properties of brake friction materials, Wear 264(3-4): 204-210. http://dx.doi.org/ 10.1016/j.wear.2007.03.004.
6. **Matějka, V.; Lu, Y.; Jiao, L.; Huang, L.; Tomášek, V.** 2010. Effects of silicon carbide particle sizes on friction-wear properties of friction composites designed for car brake lining applications, Tribology International 43(1-2): 144-151. http://dx.doi.org/ 10.1016/j.triboint.2009.05.007.
7. **Etemadi, H.; Shojaei, A.; Jahanmard, P.** 2014. Effect of alumina nanoparticle on the tribological performance of automotive brake friction materials, Journal of Rnforced Plastics &Composites 33(2): 166-178. http://dx.doi.org/ 10.1177/0731684413507011.
8. **Fei, J.; Wang, H, K.; Huang, J, F.; Zeng, X. R.; Luo, W.** 2014. Effects of carbon fiber length on the tribological properties of paper-based friction materials, Tribology International 72: 179-186. http://dx.doi.org/ 10.1016/j.triboint.2013.12.017.
9. **Su, F. H.; Zhang, Z. Z.; Guo, F.; Wang, K.; Liu, W. M.** 2006. Friction and wear of Synfluo 180XF wax and nano-Al_2O_3 filled Nomex fabric composites Mater. Materials Science and Engineering: A 430(1-2): 307-313. http://dx.doi.org/ 10.1016/j.msea.2006.05.060.
10. **La Mantia, F. P.; Morreale, M.** 2011. Green composites: a brief review, Compos Part A Composites, Part A 42(6): 579-588. http://dx.doi.org/ 10.1016/j.compositesa.2011.01.017.
11. **Zhang, X.; Li, K. Z.; Li, H. J. et al.** 2014. Tribological and mechanical properties of glass fiber reinforced paper-based composite friction material, Tribology International 69: 156-167. http://dx.doi.org/ 10.1016/j.triboint.2013.08.003.
12. **Kchaou, M.; Sellami, A.; Fajoui, J.** et al. 2018. Tribological performance characterization of brake friction materials: What test? What coefficient of friction?. Archive Proceedings of the Institution of Mechanical Engineers, Part J Journal of Engineering Tribology 233(1): 214-226. http://dx.doi.org/ 10.1177/1350650118764167.
13. **Bian, G.; Wu, H.** 2016. Friction surface structure of a C f /C–SiC composite brake disc after bedding testing on a full-scale dynamometer, Tribology International 99: 85-95. http://dx.doi.org/ 10.1016/j.triboint.2016.03.010.

14. **Kumar, M.; Bijwe, J.** 2011. Non-asbestos organic (NAO) friction composites: Role of copper; its shape and amount, Wear 270(3-4): 269-280. http://dx.doi.org/ 10.1016/j.wear.2010.10.068.
15. **Hwang, H, J.; Jung, S, L.; Cho, K, H.** 2010. Tribological performance of brake friction materials containing carbon nanotubes, Wear 268(3-4): 519-525. http://dx.doi.org/ 10.1016/j.wear.2009.09.003.
16. **Matějka, V.; Fu, Z.; Kukutschová, J.** 2013. Jute fibers and powderized hazelnut shells as natural fillers in non-asbestos organic non-metallic friction composites, Materials & Design 51: 847-853. http://dx.doi.org/ 10.1016/j.matdes.2013.04.079.
17. **Ma, Y. H.; Liu, Y. C.; Menon C.; Tong, J.** 2015. Evaluation of wear resistance of friction materials prepared by granulation, ACS Appl. Mater. Interfaces 7(41): 22814–22820. http://dx.doi.org/ 10.1021/acsami.5b04654.
18. **Kachhap, R. K.; Satapathy, B. K.** 2014. Synergistic effect of tungsten disulfide and cenosphere combination on braking performance of composite friction materials, Materials & Design 56(4): 368-378. http://dx.doi.org/ 10.1016/j.matdes.2013.11.006.
19. **Dadkar, N.; Tomar, B. S.; Satapathy, B. K.** 2010. Performance assessment of hybrid composite friction materials based on flyash–rock fibre combination, Materials & Design 31(2): 723-731. http://dx.doi.org/ 10.1016/j.matdes.2009.08.009.
20. **Tiwari, A.; Jaggi, H. S.; Kachhap, R. K.** 2014. Comparative performance assessment of cenosphere and barium sulphate based friction composites, Wear 309(1–2): 259-268. http://dx.doi.org/ 10.1016/j.wear.2013.12.001.
21. **Satapathy, B. K.; Majumdar, A.; Tomar, B. S.** 2010. Optimal design of flyash filled composite friction materials using combined Analytical Hierarchy Process and Technique for Order Preference by Similarity to Ideal Solutions approach, Materials & Design 31(4): 1937-1944. http://dx.doi.org/ 10.1016/j.matdes.2009.10.047.
22. **Gweon, J. H.; Joo, B. S.; Jang, H.** 2016. The effect of short glass fiber dispersion on the friction and vibration of brake friction materials, Wear 362–363(9): 61-67. http://dx.doi.org/ 10.1016/j.wear.2016.05.004.
23. **Kumar, M.; Bijwe, J.** 2016. NAO friction materials with various metal powders: Tribological evaluation on full-scale inertia dynamometer, Wear 269(11–12): 826-837. http://dx.doi.org/ 10.1016/j.wear.2010.08.011.
24. **Coutinho, C. P.; Baptista, A. J.; Rodrigues, J. D.** 2016. Reduced scale models based on similitude theory: A review up to 2015, Engineering Structures 119: 81-94. http://dx.doi.org/ 10.1016/j.engstruct.2016.04.016.
25. **Ramu, M.** 2013. Establishment of structural similitude for elastic models and validation of scaling laws, Ksce Journal of Civil Engineering 17(1): 139-144. http://dx.doi.org/ 10.1007/s12205-013-1216-x.
26. **Luo, Z.; Guo, J.; Zhu, Y.** 2016. Considering the requirements of static strength for the rotating straight blade similar experimental model design method, Journal of Mechanical Engineering 52(9): 79-85. http://dx.doi.org/ 10.3901/JME.2016.09.079.
27. **Wang, Y.; Huang, H.; Li, J. Q.** 2017. Experiment on lunar rover's trafficability on slope terrain based on similarity theory, Transactions of the Chinese Society for Agricultural Machinery 48(4): 406-412. http://dx.doi.org/10.6041/j.issn.1000-1298.2017.04.054.
28. **Wang, C. H.; Liu, Y.** 2017. Analysis of impact energy absorption for foam aluminum components based on similarity theory, Mechanical Science and Technology for Aerospace Engineering 36(10): 1542-1549. http://dx.doi.org/ 10.1016/j.wear.2017.04.015.
29. **Wang, Y. Y.; Zhang Z. R.** 2011. Similar experimental study of test model and prototype of vibrating screen, Journal of Mechanical Engineering 47(5): 101-105. http://dx.doi.org/ 10.3901/JME.2011.05.101.
30. **Guo, L. B.; Wang, Z. W.; Liu, T.** 2006. Similitude criteria of externally pressurized spherical gas bearing with inherent compensation, Tribology 26(3): 257-263. http://dx.doi.org/10.3321/j.issn:1004-0595.2006.03.014.
31. **Sanders, P. G.; Dalka, T. M.; Basch, R. H.** 2001. A reduced-scale brake dynamometer for friction characterization, Tribology International 34(9): 609-615. http://dx.doi.org/ 10.1016/S0301-679X(01)00053-6.
32. **Zhao, X. L.; Wang, T. S.; Cheng, G. M.** 2007. The scaling 1:5 dynamometer based on similar principle for friction material and its comparability analysis, Lubrication Engineering 32(5): 153-156 (in Chinese). http://dx.doi.org/10.3969/j.issn.0254-0150.2007.05.045.
33. **Ma, J. J.; Zhao J. X.; Liu, X. Y.** 2016. Research on subscale inertia test equipment and test procedure of vehicle friction materials, Lubrication Engineering 41(7): 102-106. http://dx.doi.org/10.3969/j.issn.0254-0150.2016.07.018.
34. **Wang, X. L.; Yang, J. Y.; Gao, F.** 2019. Research on the reduced-scale model of railway braking pair based on similarity theory, Lubrication Engineering 44(3): 80-85+90 (in Chinese). http://dx.doi.org/10.3969/j.issn.0254-0150.2019.03.013.
35. **Liu, Y.; Ma, Y.; Yu, J.** 2018. Development and characterization of alkali treated abaca fiber reinforced friction composites, Composite Interfaces (4): 1-16. http://dx.doi.org/ 10.1080/09276440.2018.1472456.

Zhenyu WANG, Jie WANG, Lining WANG, Yunhai MA

DEVELOPMENT AND COMPARATIVE EVALUATION OF REDUCED-SCALE KRAUSS FRICTION TESTER BASED ON SIMILARITY THEORY

S u m m a r y

Based on the similarity principle, the basic parameters of the reduced-scale Krauss tester were derived from the full-scale Krauss tester by using the dimensional analysis method. The main structure of the Krauss testing machine had been made, and some components and parts such as brake system, servo loading system and torque measuring system had been designed and manufactured. The same

batch and molded NAO brake friction material had been rigorously evaluated on two Krauss testers following ECE R-90 procedure as per the ‘‘Economic Commission for Europe” (ECE) regulations and these parameters such as friction torque, brake pressure, friction coefficient, test temperature and time had been discussed. The results showed that the reduced-scale Krauss tester was faster response than that of the full-scale Krauss tester in the process of brake growth and brake release, the brake completion time was about 370 ms ahead of schedule. However, the full-scale Krauss tester had a slower response and the brake completion time delay was about 240 ms. During the entire test, the average coefficient of friction was closer and the relative error is 6.3%, and the maximum and minimum values of the friction coefficient appeared at the same brake sequence, test section and brake cycle. The test temperature had good linear correlation in the whole test process. The total test time for reduced-scale Krauss tester was about 4/5 of full-scale Krauss tester. In each test, if the same other conditions existed, the power cost of the reduced-scale Krauss tester is 20.79 % of the power cost of the full-scale Krauss tester when the ECE R-90 test program was executed. From the comparison of the main test indexes, the test data of the scaled Krauss test machine reflected the fluctuation and correlation of the test data of the full-scale Krauss test machine to a certain extent, providing a new test equipment for the brake friction material.

Keywords: similarity theory, Krauss tester, friction material, comparative test, development.

Received September 09, 2019
Accepted August 24, 2022